Contribution from the Département de chimie,
Université de Sherbrooke, Sherbrooke, Quebec, Canada J1K 2R1

Preparation of Novel Palladium(I)-Palladium(I) Bonded Complexes, $Pd_2(diiso)_2X_2$ (diiso: dmb = 1,8-Diisocyano-*p*-menthane, tmb = 2,5-Dimethyl-2,5-diisocyanohexane) (X = Cl, Br), and Their Photoinduced Oxidative Addition Reactivities toward Chlorocarbons. Crystal and Molecular Structures of $Pd_2(dmb)_2Cl_4 \cdot H_2O$, $Pd_2(tmb)_2Cl_4 \cdot 2CH_3CN$, and $Pd_2(dmb)_2Br_2Cl_2$

Daniel Perreault, Marc Drouin, Andrê Michel,*[1] and Pierre D. Harvey*

Received September 20, 1991

New palladium(I)-palladium(I) bonded complexes, $Pd_2(diiso)_2X_2$ (diiso = dmb (1,8-diisocyano-*p*-menthane) and tmb (2,5-dimethyl-2,5-diisocyanohexane); X = Cl, Br), have been prepared by direct reaction of $Pd_2(dba)_3$ (dba = dibenzylideneacetone) with $Pd_2(diiso)_2X_4$ and diiso in a 1:1:2 stoichiometric amount. The yellow-orange products have been characterized by ^1H NMR, IR, and UV-visible spectroscopy and fast atom bombardment mass spectrometry. Evidence for the Pd-Pd bond is provided by the UV-visible spectra, exhibiting intense absorption in the 400-500 nm range, and by the Raman spectra of the $Pd_2(diiso)_2Cl_2$ complexes, in which $\nu(Pd_2)$ is found in the 172-174 cm^{-1} range. The complexes photoreact readily in CH_2Cl_2 and $CHCl_3$ solutions to afford the corresponding oxidative addition products, the nonmetal-metal-bonded $Pd_2(diiso)_2X_2Cl_2$ compounds (X = Cl, Br), with photochemical quantum yields (Φ) ranging from 0.05 to 1.35. The Φ values increase from X = Cl to X = Br and from CH_2Cl_2 to $CHCl_3$ and when the dmb bridging ligand is used instead of tmb. The enhanced reactivity of the dmb complexes could be associated with the presence of ring stress. The compounds $Pd_2(dmb)_2Cl_4 \cdot H_2O$, $Pd_2(tmb)_2Cl_4 \cdot 2CH_3CN$, and $Pd_2(dmb)_2Br_2Cl_2$ have been characterized by X-ray crystallography. Crystal data: $Pd_2(dmb)_2Cl_4 \cdot H_2O$, monoclinic $P2_1/n$, a = 9.2357 (7) Å, b = 14.7287 (8) Å, c = 11.8082 (11) Å, β = 94.635 (3)°, V = 1601.01 (8) Å^3, Z = 2; $Pd_2(tmb)_2Cl_4 \cdot 2CH_3CN$, triclinic, $P\bar{1}$, a = 8.929 (4) Å, b = 10.6958 (17) Å, c = 10.7386 (19) Å, α = 70.152 (15)°, β = 66.47 (3)°, γ = 72.260 (22)°, V = 867.2 (4) Å^3, Z = 1; $Pd_2(dmb)_2Cl_2Br_2$: monoclinic $P2_1/n$, a = 9.4112 (3) Å, b = 14.9123 (8) Å, c = 11.4053 (8) Å, β = 94.989 (3)°, V = 1594.6 (1) Å^3, Z = 2.

Introduction

The photochemistry of metal-metal bonds has attracted a large amount of interest over the past 20 years.[2,3] The main feature is the photoinduced homolytic cleavage of the metal-metal bond, producing mononuclear species that are highly reactive with respect to oxidative addition and substitution reactions;[3] classic examples involve d^7-d^7 singly bonded homo- and heterobinuclear complexes.[2,3] Curiously, very few photochemical studies on the unbridged and unsaturated electron-rich d^9-d^9 singly bonded dimers have been reported.[4,5] In all cases, the photoproducts are either oxidized or reduced mononuclear compounds.

We wish to report the synthesis of novel bridged Pd(I)-Pd(I) bonded complexes, $Pd_2(diiso)_2X_2$ (diiso = tmb, dmb; X = Cl, Br), and their photooxidative addition reactivities toward chlorocarbons (CH_2Cl_2 and $CHCl_3$). We chose the tmb and dmb bridging ligands because the long diisocyanide bite distances reduce the possibility of forming the frequently encountered A-frame products (as is the case for the $M_2(dppm)_2X_2$ complexes (M = Pd, Pt; X = Cl, Br, I)).[6] In this work, it will be shown that the $Pd_2(diiso)_2X_2$ complexes photoreact readily in CH_2Cl_2 and $CHCl_3$ solutions to form the nonmetal-metal-bonded $Pd_2(diiso)_2X_2Cl_2$ complexes, via presumably a halogen atom abstraction mechanism, and that the choice of bridging ligand (tmb or dmb) also influences the photochemical quantum yields for the homolytic M_2-bond cleavage reaction.

Experimental Section

Materials. $PdCl_2$ and $PdBr_2$ (Strem Chemical Co.) were used as received. The solvents CH_3CN, C_6H_6, CH_2Cl_2, and $CHCl_3$ (Aldrich Chemical Co.) were purified according to standard procedures.[7] $Pd_2(dba)_3$ (dba = dibenzylideneacetone),[8] tmb, and dmb (yield 50-80%)[9] were prepared according to literature procedures. CD_3CN and $CDCl_3$ (Aldrich) were used as received. All syntheses were carried out under inert atmosphere at room temperature. The solutions were freshly prepared in the dark and kept away from daylight prior to all spectroscopic measurements to ensure that no photochemical reaction occurs during the experiment.

Instruments. The FT-IR (4000-200 cm^{-1}) spectra were obtained on a Bomem (MB-102) spectrometer. NMR spectra were measured on a Bruker WM250 spectrometer. The mass spectra were acquired using a Kratos MS-50 TCTA spectrometer using an Iontech Saddle Field Source Model FAB 11NF operating at 70 kV with 2 mA current. The samples were in thiolglycerol matrices. UV-visible spectra were obtained on a Hewlett Packard (HP 8452A) diode array spectrophotometer. The elemental analyses were performed by Guelph Chemical Laboratories, Ltd. (Guelph, Ontario) (C/H/N), and in our department using a KEVEX-700 X-ray emission spectrofluorometer operating at 60 kV (Pd/Cl/Br).

Raman Spectra. The 298 K solid-state Raman spectra were obtained on three different spectrometers so that various excitation wavelengths could be employed. The first instrument was an ISA microRaman Jobin-Yvon U-1000 spectrometer using the 488.0-, 514.5-, and 647.1-nm lines of Spectra Physics argon and krypton ion lasers for excitation. Typically, the laser power was 5 mW at the samples, using a 32× microscope, with 300-μm slits. No smoothing was performed. The second instrument was a microRaman Spex Triplemate system, with 600 grooves/mm gratings, 500 mm blaze, using a Lexel Raman ion laser (752 nm excitation) and a 40× microscope with a 0.6 NA objective. The spectra were recorded with 2-, 6-, and 0.2-mm slits, 10 scans, and no smoothing. The third instrument was a Perkin-Elmer FT-IR/FT-Raman spectrometer using a Spectron 3.5-W Nd:YAG laser (1064 nm). Typically, 100 scans were accumulated with a resolution of 4 cm^{-1}. The measured relative intensities of the $\nu(Pd_2)$ bands were ratioed against the intensities of the $\nu(CH)$ bands (~2930 cm^{-1}) of the bridging ligands in order to follow selective preresonance enhancement.

Photochemical Studies. The photochemical reactions were performed using a Photon Technology Int. (PTI) Hg-Xe 200-W arc lamp and a LPS-250 power supply (PTI). The light was filtered using Oriel optical cutoff filters, no. 51470 (390 nm cutoff). The photochemical quantum yield measurements were performed using the ferrioxalate actinometry

(1) Correspondence pertaining to the crystallography results should be addressed to this author.
(2) Meyer, T. J.; Caspar, J. V. *Chem. Rev.* **1985**, *85*, 187.
(3) Geoffroy, G. L.; Wrighton, M. S. *Organometallic Photochemistry*; Academic Press: New York, 1979.
(4) (a) Metcalf, P. A.; Kubiak, C. P. *J. Am. Chem. Soc.* **1986**, *108*, 4682. (b) Lemke, F. R.; Granger, R. M.; Morgenstern, D. A.; Kubiak, C. P. *J. Am. Chem. Soc.* **1990**, *112*, 4052.
(5) Yamamoto, Y.; Yamazaki, H. *Bull. Chem. Soc. Jpn.* **1985**, *58*, 1843.
(6) (a) Puddephatt, R. J. *Chem. Soc. Rev.* **1983**, *12*, 99. (b) Balch, A. L. *Adv. Chem. Ser.* **1982**, *196*, 243. (c) Kubiak, C. P.; Eisenberg, R. *J. Am. Chem. Soc.* **1977**, *99*, 6129.
(7) Perrin, D. D.; Armarego, W. L. F.; Perrin, D. R. *Purifications of Laboratory Chemicals*; Pergamon: Oxford, 1966.
(8) Takahashi, Y.; Ito, T.; Ishi, Y. *J. Chem. Soc., Chem. Commun.* **1970**, 1065.
(9) Weber, W. P.; Gokel, G. W.; Ugi, I. K. *Angew. Chem., Int. Ed. Engl.* **1972**, *11*, 530.

0020-1669/92/1331-2740$03.00/0

method.[10] The spectrometer used for monochromatic excitation was an Aminco-Bowman instrument equipped with a single monochromator and a 200-W Hg–Xe lamp (Hanovia). The slits were set at 0.5 mm, and excitation was at 405 nm for all samples and standards. The absorbance of the complex solutions was adjusted to a value of 1 (at 405 nm) prior to the photochemical quantum yield measurements. This adjustment was done by weighing the samples and dissolving them in a known amounts of solvent. Typical concentrations range from 1×10^{-4} to 4×10^{-4} M. The calibrations of the standard ferrioxalate actinometric solutions were performed carefully in the dark. The absorbance change at a given irradiation time was followed by UV–visible spectroscopy (Hewlett-Packard 8452A) at λ_{max} 448, 420, 446, and 420 nm for $Pd_2(dmb)_2Cl_2$, $Pd_2(tmb)_2Cl_2$, $Pd_2(dmb)_2Br_2$, and $Pd_2(tmb)_2Br_2$, respectively. All measurements and calibration experiments were performed at least 3 times and made before 10% photoconversion. The quantum yields were corrected for incomplete absorption.

Synthesis: $Pd_2(diiso)_2X_4$ Complexes (X = Cl, Br). (a) $Pd_2(dmb)_2Cl_4$. To a 25 mL aqueous $PdCl_2$ solution (3.4 mmol), 10.4 mmol of NaCl and 3.8 mmol of dmb were added. The mixture was stirred for 2 h; a pale yellow solid precipitated. The crude solid was filtered and washed with water. The solid was slowly recrystallized from acetonitrile/diethyl ether solution (70–80% yield), which afforded crystals suitable for X-ray crystallographic analysis. The product was identified as $Pd_2(dmb)_2Cl_4 \cdot H_2O$ from the X-ray results. ^1H NMR (250 MHz, $CDCl_3$): (δ = 1.09 (m), 1.31 (m), 1.49 (m), 1.65 (m) ppm, IR (CsI): 2240 (ν(NC)), 2199 (ν(NC)), 338 cm^{-1} (ν(PdCl)); UV–visible (CH_3CN): λ_{max} (ϵ) 294 (3310), 224 nm (10 570 M^{-1} cm^{-1}).

(b) $Pd_2(tmb)_2Cl_4$. $Pd_2(tmb)_2Cl_4$ was synthesized and purified in the same way as $Pd_2(dmb)_2Cl_4$, except tmb was used instead of dmb (70–80% yield). The compound was identified by X-ray crystallography as $Pd_2(tmb)_2Cl_4 \cdot 2CH_3CN$. ^1H NMR (CD_3CN): δ = 1.36 (s), 1.49 (s), 1.58 (m), 1.65 (m) ppm, IR (CsI): 2249 (ν(NC)), 322 (ν(PdCl)), 341 cm^{-1} (ν(PdCl)); UV–visible (CH_3CN): λ_{max} (ϵ) 316 (440), 204 nm (9350 M^{-1} cm^{-1}).

(c) $Pd_2(dmb)_2Br_4$. To a 25 mL aqueous $PdBr_2$ solution (1.0 mmol), 3.0 mmol of KBr and 1.3 mmol of dmb were added. The mixture was stirred for 2 h. A yellow precipitate settled out. The crude solid was filtered and washed with water. Recrystallization from acetonitrile/diethyl ether afforded a yellow product (70–80% yield). There was no evidence for solvation in the solid state from IR spectroscopy and chemical analysis. Anal. Calcd for $C_{24}H_{36}N_4Br_4Pd_2$: C, 31.57; H, 6.13; N, 3.94; Br, 35.01; Pd, 23.31. Found: Br, 34.71; Pd, 22.99. ^1H NMR ($CDCl_3$): δ = 1.10 (m), 1.31 (m), 1.38 (s), 1.45 (m), 1.65 (m) ppm. IR (CsI): 2232 (ν(NC)), 2147 (ν(NC)), 222 cm^{-1} (ν(PdBr)). UV–visible (CH_3CN): λ_{max} (ϵ) 228 (45 500), 262 (17 340), 302 nm (2850 M^{-1} cm^{-1}).

(d) $Pd_2(tmb)_2Br_4$. $Pd_2(tmb)_2Br_4$ was synthesized and purified in the same way as $Pd_2(dmb)_2Br_4$, except tmb was used instead of dmb (70–80% yield). Anal. Calcd for $C_{20}H_{32}N_4Br_4Pd_2$: C, 27.90; H, 3.75; N, 6.51; Br, 37.13; Pd, 24.72. Found: C, 27.90; H, 3.65; N, 6.34; Br, 37.2; Pd, 24.6. ^1H NMR ($CDCl_3$): δ = 1.41 (m), 1.59 (s), 1.66 (m) ppm. IR (CsI): 2239 (ν(NC)), 2135 (ν(NC)), 227 cm^{-1} (ν(Pd–Br)). UV–visible: λ_{max} (ϵ) ~238 (7110); shoulder, 302 nm (475 M^{-1} cm^{-1}).

$Pd_2(diiso)_2X_2$ Complexes (X = Cl, Br). (a) $Pd_2(dmb)_2Cl_2$. A 0.55-mmol quantity of $Pd_2(dba)_3 \cdot C_6H_6$ was dissolved in ~25 mL of benzene. To this solution was added dropwise a 10-mL solution containing 0.55 mmol of $Pd_2(dmb)_2X_4$ and 1.2 mmol of dmb under inert atmosphere. The dark purple color disappeared and an orange solid precipitated within minutes. The crude solid was filtered and washed with portions of benzene and was recrystallized twice from an acetonitrile/diethyl ether solution (40–50% yield). Anal. Calcd for $C_{24}H_{36}N_4Cl_2Pd_2$: C, 43.40; H, 5.46; N, 8.44; Cl, 10.68; Pd, 32.03. Found: C, 43.31; H, 5.40; N, 8.80; Cl, 10.91; Pd, 32.31. Mass spectrum (FAB), *m/e* 626 ($Pd_2(dmb)_2Cl^{•+}$), 594 ($Pd_2(dmb)_2^{•+}$). IR (CsI): 2232 (ν(NC)), 2170 (ν(NC)), 330 cm^{-1} (ν(PdCl)). ^1H NMR (CD_3CN): δ_{ppm} = 1.10 (d), 1.29 (m), 1.54 (m), 1.66 (s). UV–visible (CH_3CN): λ_{max} (ϵ) 264 (45 500), 316 (2990), 448 nm (9970 M^{-1} cm^{-1}).

(b) $Pd_2(tmb)_2Cl_2$. $Pd_2(tmb)_2Cl_2$ was synthesized and purified in the same way as $Pd_2(dmb)_2Cl_2$, except $Pd_2(tmb)_2Cl_4$ was used instead of $Pd_2(dmb)_2Cl_4$ (40–50% yield). Anal. Calcd for $C_{20}H_{32}N_4Cl_2Pd_2$: C, 39.24; H, 5.27; N, 9.15; Cl, 11.59; Pd, 34.79. Found: C, 39.35; H, 5.30; N, 9.14; Cl, 11.71; Pd, 34.77. ^1H NMR (CD_3CN): δ = 1.10 (d), 1.30 (m), 1.50 (m), 1.66 (s) ppm. IR (CsI): 2186 (ν(NC)), 330 cm^{-1} (ν(PdCl)). UV–visible (CH_3CN): λ_{max} (ϵ) 220 (9690), 266 (5880), 316 (3900), 420 nm (3860 M^{-1} cm^{-1}).

(c) $Pd_2(dmb)_2Br_2$. $Pd_2(dmb)_2Br_2$ was synthesized and purified in the same way as $Pd_2(dmb)_2Cl_2$, except $Pd_2(dmb)_2Br_4$ was used instead of $Pd_2(dmb)_2Cl_4$ (40–50% yield). Anal. Calcd for $C_{24}H_{36}N_4Br_2Pd_2$: C, 38.27; H, 4.82; N, 7.44; Br, 21.22; Pd, 28.23. Found: C, 38.28; H, 4.80; N, 7.40; Br, 21.41; Pd, 28.45. Mass spectrum (FAB), *m/e* 753 ($Pd_2(dmb)_2Br_2^{•+}$), 673 ($Pd_2(dmb)_2Br^{•+}$), 594 ($Pd_2(dmb)_2^{•+}$). ^1H NMR (CD_3CN): δ = 1.09 (d), 1.19 (m), 1.28 (s), 1.55 (m) ppm. IR (CsI): 2230 (ν(NC)), 2168 (ν(NC)). UV–visible (CH_3CN): λ_{max} (ϵ) 224 (16 200), 262 (6360), 328 (2780), 446 nm (6290 M^{-1} cm^{-1}).

(d) $Pd_2(tmb)_2Br_2$. $Pd_2(tmb)_2Br_2$ was synthesized and purified in the same way as $Pd_2(dmb)_2Cl_2$, except $Pd_2(tmb)_2Br_4$ was used instead of $Pd_2(dmb)_2Cl_4$ (40–50% yield). Anal. Calcd for $C_{20}H_{32}N_4Br_2Pd_2$: C, 34.26; H, 4.60; N, 7.99; Br, 22.79; Pd, 30.35. Found: C, 34.49; H, 4.94; N, 8.03. ^1H NMR (CD_3CN): δ = 1.21 (s), 1.35 (m), 1.53 (m) ppm. IR (CsI): 2226 (ν(NC)), 2172 (ν(NC)). UV–visible: λ_{max} (ϵ) 270 (20 400), 328 (9840), 420 nm (3130 M^{-1} cm^{-1}).

Photosynthesis. (a) $Pd_2(dmb)_2Br_2Cl_2$. Either CH_2Cl_2 or $CHCl_3$ solutions of $Pd_2(dmb)_2Br_2$ were put in glass vessels and broad band irradiated with $\lambda > 390$ nm. The photoreactions were monitored by UV–visible spectroscopy. At the end of the reaction (about 3 h), the solvent was evaporated and the yellow solid obtained was recrystallized from an acetonitrile/diethyl ether solution. The identity of the photoproduct was confirmed by X-ray crystallography, for which suitable crystals were obtained by slow evaporation of acetonitrile solutions. Anal. Calcd for $C_{24}H_{36}N_4Br_2Cl_2Pd_2$: Br, 19.39; Cl, 8.60; Pd, 25.82. Found: Br, 19.30; Cl, 8.71; Pd, 25.67. ^1H NMR (CD_3CN) δ = 1.33 (m), 1.55 (m) ppm. IR (CsI): 2240 (ν(NC)), 343 (ν(PdCl)), 226 cm^{-1} (ν(PdBr)). UV–visible: λ_{max} (ϵ) 220 (28 200), 296 nm (4140 M^{-1} cm^{-1}).

(b) $Pd_2(tmb)_2Br_2Cl_2$. $Pd_2(tmb)_2Br_2Cl_2$ was prepared in the same way as described for $Pd_2(dmb)_2Br_2Cl_2$ except $Pd_2(tmb)_2Br_2$ was used instead of $Pd_2(dmb)_2Br_2$. Anal. Calcd for $C_{20}H_{32}N_4Br_2Cl_2Pd_2$: Br, 20.70; Cl, 9.18; Pd, 27.56. Found: Br, 20.53; Cl, 9.31; Pd, 25.49. IR (CsI): 2249 (ν(NC)), 335 (ν(PdCl)), 228 cm^{-1} (ν(PdBr)). UV–visible: λ_{max} (ϵ) 226 (15 400), 292 nm (1320 M^{-1} cm^{-1}). ^1H NMR (CD_3CN): δ = 1.36 (m), 1.53 (m) ppm.

(c) $Pd_2(dmb)_2Cl_4$ and $Pd_2(tmb)_2Cl_4$. Either CH_2Cl_2 or $CHCl_3$ solutions of $Pd_2(dmb)_2Cl_2$ or $Pd_2(tmb)_2Cl_2$ were put in glass vessels and broad band irradiated with $\lambda > 390$ nm. The procedures were the same as stated for $Pd_2(dmb)_2Br_2Cl_2$. The photoproducts were unambiguously identified as $Pd_2(dmb)_2Cl_4$ and $Pd_2(tmb)_2Cl_4$ oxidized complexes from the comparison of the ^1H NMR, IR, and UV–vis data and by chemical analysis.

Crystallography. Crystal data and details of data collection and refinement procedures are summarized in Table I for $Pd_2(dmb)_2Cl_4 \cdot H_2O$, $Pd_2(dmb)_2Cl_2Br_2$, and $Pd_2(tmb)_2Cl_4 \cdot 2(CH_3CN)$. Data were collected at 298 K on an Enraf Nonius diffractometer using graphite-monochromatized Mo Kα radiation (λ = 0.710 73 Å). Intensities were corrected for Lorentz and polarization effects. A spherical absorption correction was applied for $Pd_2(dmb)_2Cl_4$ and $Pd_2(dmb)_2Br_2Cl_2$ but not for $Pd_2(tmb)_2Cl_4$. The NRCVAX system[11a] was used for all calculations; these were done on an IBM RISC 6000 for $Pd_2(dmb)_2Cl_4$ and $Pd_2(dmb)_2Br_2Cl_2$ and on a MicroVAX 2000 for $Pd_2(tmb)_2Cl_4$. The structures were solved using direct methods. Hydrogen positions were computed for $Pd_2(dmb)_2Cl_4$ and $Pd_2(dmb)_2Br_2Cl_2$. $Pd_2(dmb)_2Cl_4$ and $Pd_2(dmb)_2Br_2Cl_2$ crystallize on centers of symmetry and the dmb ligands are disordered; the occupancy parameter refined to [0.562] for one orientation and [1-0.562] for the other for $Pd_2(dmb)_2Cl_4$ and to [0.514] and [1-0.514] for $Pd_2(dmb)_2Br_2Cl_2$. The disorder results in the superimposition of C2, C4, C6, and C8 with occupancies fixed at 1. Those atoms were set to be anisotropic, whereas C3, C5, C7, C10, C11, and C12 and their corresponding disordered atoms were set to be isotropic for the refinement procedure. We found that our model for the representation of the disordered ligand was not perfect, resulting in large deviations of the distances and angles from the expected values. The two Cl atoms show large thermal motions especially for Cl1. The C12 atom presents one long non-bonding interaction (3.473 (3) Å) with the equivalent Pd atom at $2-x, 1-y, -z$ (structure I). One water molecule was located by Fourier difference at 3.268 (10) Å from Cl1 and 3.215 (10) Å of Cl2, which are in good range for H-bonding as viewed in the packing diagram (see text below). Hydrogen atoms of the water molecule were not located. The final difference map shows residual electron densities in the vicinity of the Pd atom but they are less than ±1.0 e $Å^{-3}$. In $Pd_2(dmb)_2Br_2Cl_2$, the bromide and chloride atom ratio was set to 50:50 based on previous elementary analyses, their positional and thermal parameters were refined using dual scattering factors on the two single sites. Pd_2-

(10) Calvert, J. G.; Pitts, J. N. *Photochemistry*; Wiley: New York, 1966; p 783.

(11) (a) Gabe, E. J.; Lee, F.; Le Page, Y. The NRCVAX Crystal Structure System. In *Crystallographic Computing 3: Data Collection, Structure Determination, Proteins and Databases*; Sheldrick, G. M., Krüger, C., Goddard, R., Eds.; Clarendon Press: Oxford, 1985; Vol. 167. (b) Cromer, D. T.; Waber, J. T. In *International Tables for X-ray Crystallography*; Kynoch Press: Birmingham, (Present distributor Kluwer Academic Publishers: Dordrecht), 1974; Vol. IV, pp 99–101.

Table I. Crystallographic Data for $Pd_2(dmb)_2Cl_4 \cdot H_2O$, $Pd_2(tmb)_2Cl_4 \cdot 2CH_3CN$, and $Pd_2(dmb)_2Br_2Cl_2$

	$Pd_2(dmb)_2Cl_4 \cdot H_2O$	$Pd_2(tmb)_2Cl_4 \cdot 2CH_3CN$	$Pd_2(dmb)_2Br_2Cl_2$
formula	$C_{24}H_{38}N_4OCl_4Pd_2$	$C_{22}H_{38}N_6Cl_4Pd_2$	$C_{24}H_{36}N_4Cl_2Br_2Pd_2$
formula wt.	753.20	741.20	824.09
*F*000	755.92	371.95	807.89
space group	$P2_1/n$	$P\bar{1}$	$P2_1/n$
cryst syst	monoclinic	triclinic	monoclinic
a, Å	9.2357 (7)	8.929 (4)	9.4112 (3)
b, Å	14.7287 (8)	10.6958 (17)	14.9123 (8)
c, Å	11.8082 (11)	10.7386 (19)	11.4053 (5)
α, deg	90	70.152 (15)	90
β, deg	94.635 (3)	66.47 (3)	94.989 (3)
γ, deg	90	72.260 (22)	90
Z	2	1	2
T, K	298	298	298
λ, Å	0.71073	0.71073	0.71073
ρ_{calc}, g/cm^3	1.562	1.419	1.716
μ, cm^{-1}	14.68	13.54	37.84
transmission coeff	0.719–0.721		0.437–0.444
$R(F_o)^a$	0.054	0.042	0.064
$R_w{}^b$	0.052	0.024	0.059

$^a F(F_o) = \sum(F_o - F_c)/\sum(F_o)$. $^b R_w = [\sum(w(F_o - F_c)^2)/\sum(wF_o^2)]^{1/2}$.

Table II. Selected Bond Distances (Å) and Angles (deg)

$Pd_2(dmb)_2Cl_4 \cdot H_2O$		$Pd_2(tmb)_2Cl_4 \cdot 2CH_3CN$		$Pd_2(dmb)_2Br_2Cl_2$	
Pd–Cl(1)	2.478 (7)	Pd–Cl(1)	2.297 (2)	Pd–Br	2.407 (3)
Pd–Cl(2)	2.390 (3)	Pd–Cl(2)	2.282 (2)	Pd–Cl	2.408 (3)
Pd–C(1)	1.977 (9)	Pd–C(1)	1.885 (7)	Pd–C(1)	2.02 (2)
Pd–C(9)	1.964 (9)	Pd–C(6)	1.935 (7)	Pd–C(9)	1.964 (15)
N(1)–C(1)	1.126 (11)	N(1)–C(1)	1.153 (9)	N(1)–C(1)	1.11 (2)
N(2)–C(9)	1.135 (11)	N(2)–C(6)	1.132 (8)	N(2)–C(9)	1.09 (2)
Pd–Pd(a)	4.3996 (14)			Pd–Pd(a)	4.466 (2)
Pd–Cl(2)a	3.468 (3)			Pd–Br(a)	3.662 (2)
Cl(2)–OW	3.221 (10)				
Cl(1)–OW	3.267 (10)				
Cl(1)–Pd–Cl(2)	178.61 (12)	Cl(1)–Pd–Cl(2)	93.62 (8)	Br–Pd–Cl	177.23 (12)
Cl(1)–Pd–C(1)	88.6 (3)	Cl(1)–Pd–C(1)	85.4 (2)	Br–Pd–C(1)	89.8 (5)
Cl(1)–Pd–C(9)	91.4 (3)	Cl(1)–Pd–C(6)	177.7 (3)	Br–Pd–C(9)	88.1 (5)
Cl(2)–Pd–C(1)	90.3 (3)	Cl(2)–Pd–C(1)	179.0 (2)	Cl–Pd–C(1)	92.5 (5)
Cl(2)–Pd–C(9)	89.7 (3)	Cl(1)–Pd–C(6)	95.5 (3)	Cl–Pd–C(9)	89.6 (5)
Pd–C(1)–N(1)	178.2 (8)	Cl(2)–Pd–C(6)	85.53 (2)	Pd–C(1)–N(1)	178.5 (15)
Pd–C(9)–N(2)	179.0 (8)			Pd–C(9)–N(2)	177.0 (2)

$(tmb)_2Cl_4$ crystallizes on centers of symmetry. All H atoms were located by Fourier differences and refined, except the acetonitrile hydrogen atoms, which were computed and not refined. No disorder is observed in the tmb ligand. Atomic scattering factors as stored in the NRCVAX program are those of Cromer and Waber.[11b] Final values for the atomic parameters are given as supplementary material.

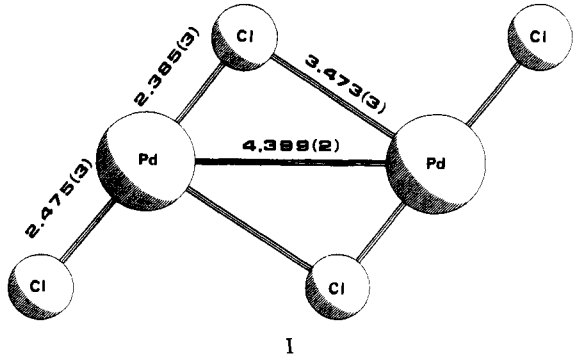

I

Results and Discussion

$Pd_2(diiso)_2X_4$ Complexes. The d^8–d^8 compounds are obtained in good yield (70–80%) from the reactions between PdX_2 (X = Cl, Br) and the diisocyanide ligands in the presence of the corresponding NaX salt. The dmb and tmb complexes are obtained as the trans,trans and cis,cis isomers, respectively, as found from single-crystal X-ray analysis (Figures 1 and 2, Table II). The monohydrated $Pd_2(dmb)_2Cl_4$ is isostructural to $Pd_2(dmb)_2I_4$[12] and consists of two tetracoordinated Pd atoms in a square-planar configuration placed face-to-face, with the dmb bridging ligands adopting a trans configuration with respect to each other. The Pd_2 distance is 4.399 (2) Å so that M_2 interactions are expected to be very weak.[13] The head-to-tail and head-to-head isomers are possible, but the solution ^1H NMR and X-ray diffraction studies in this work (T = 293 K) did not allow us to clearly distinguish between the two in this work. The Cl atoms do not bridge the Pd atoms, but two of the Cl atoms interact weakly with the adjacent Pd atom (structure I, r(Pd–Cl) = 3.473 (3) Å). The Pd atoms in the $Pd_2(tmb)_2Cl_4$ structure are also tetracoordinated in a square-planar configuration (cis isomer). It is not clear why the dmb and tmb ligands adopt different configurations; interligand steric interactions may be at the origin of the difference.[14]

(12) Che, C.-M.; Herbstein, F. H.; Schaefer, W. P.; Marsh, R. E.; Gray, H. B. *Inorg. Chem.* **1984**, *23*, 2572.

(13) (a) Unpublished results for $Rh_2(dmb)_4^{2+}$ show that $r(Rh_2)$ = 4.4 Å with $\nu(Rh_2)$ = 26 cm^{-1}.[13b] Such distances and frequencies are similar to those of the van der Waals dimers (He_2, Ne_2, Ar_2, etc.).[13c] (b) Miskowski, V. M., unpublished results. (c) Huber, K. P.; Herzberg, G. *Molecular Spectra and Molecular Structure Constants of Diatomic Molecules*; Van Nostrand: New York, 1979. (d) The X-ray analysis shows that the dmb ligands are disordered and the $Pd_2(dmb)_2Cl_4$ molecule sits on a crystallographic center of inversion. This situation precludes any definitive structural conclusion on the head-to-tail and head-to-head isomerism. A recent study on asymmetric $[Ir_2(dmb)_4(PPh_3)(AuPPh_3)]^{3+}$ complex reported by Sykes and Mann[13e] demonstrates this phenomenon. (e) Sykes, A. G.; Mann, K. R. *J. Am. Chem. Soc.* **1990**, *112*, 7247, and references therein.

(14) (a) In the *cis*-$(C_6H_{11}NC)_2PdCl_2$ structure[14b] one cyclohexyl group is oriented perpendicular to the PdL_4 plane, and the other is oriented parallel to the plane but away from the first cyclohexyl. The authors suggested that intercyclohexyl steric interactions could be responsible for this phenomenon. (b) Kinato, Y.; Hori, T. *Acta Crystallogr.* **1981**, *B37*, 1919.

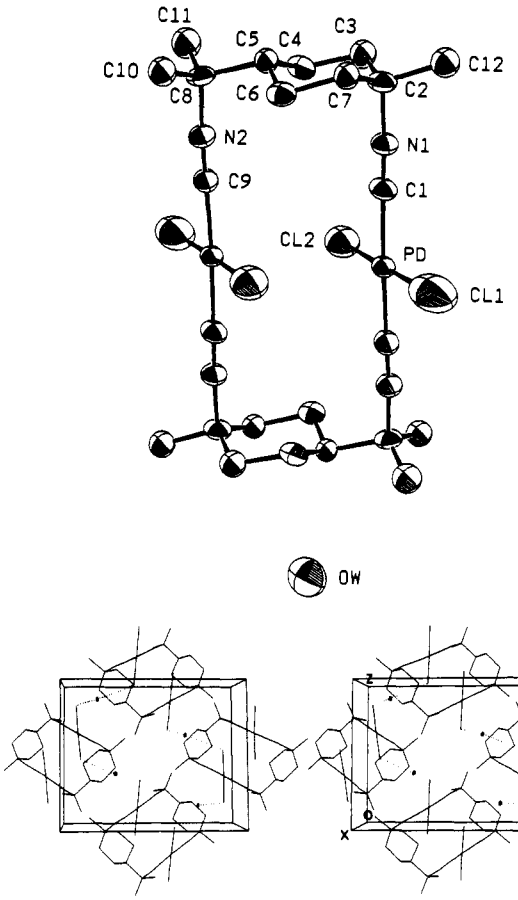

Figure 1. (Top) Molecular structure and atom labeling of *trans,trans*-$Pd_2(dmb)_2Cl_4 \cdot H_2O$, showing 50% probability ellipsoids. For clarity, the hydrogen atoms have been omitted. (Bottom) Crystal packing showing the H-bond interactions between the Cl1 atoms and the water molecules. The oxygen atoms are represented by the dots (●).

$Pd_2(tmb)_2Cl_4$ crystallizes in an anti-geometry similar to that of $Au_2(tmb)Cl_2$[15] with an intramolecular r(Pd–Pd) of ~6 Å. The crystal packing forces the square-planar moieties to stack in a quasi-linear fashion[16] with no Pd_2 interaction (Figure 3). This packing phenomenon is not unique; a recent report on the crystal structure of *cis*-$(2,6\text{-}C_6H_3(CH_3)_2NC)_2PdCl_2$ has shown a similar behavior, where the r(Pd–Pd) values range from 4.0 to 4.2 Å.[17] The Pd–Cl and Pd–C distances in $Pd_2(dmb)_2Cl_4$ (2.48 and 2.39 and 1.98 and 1.96 Å) are longer than those found in $Pd_2(tmb)_2Cl_4$ (2.30 and 2.28 and 1.89 and 1.94 Å), reflecting the trans effect in the $Pd_2(dmb)_2Cl_4$ compound. The N≡C (1.13–1.15 Å), C—C, and C—H bond distances are all normal for both complexes, and there is no major deviation from the ideal 90° 4-coordination geometry around the Pd atoms.[13,14,17]

$Pd_2(diiso)_2X_2$ Complexes. The air-stable yellow and orange $Pd_2(diiso)_2X_2$ compounds are prepared in reasonable yield (50–60%) via direct reactions of $Pd_2(diiso)_2X_4$ (X = Cl, Br) and $Pd_2(dba)_3$ in stoichiometric amounts in the presence of an excess of the corresponding diisocyanide bridging ligand under inert atmosphere (Scheme I). The $Pd_2(diiso)_2I_2$ compounds have been prepared but not isolated. These reactions (shown in Scheme I) give a mixture of products, some of which are air- and light-sensitive. Also, all attempts to obtain crystals suitable for X-ray analysis uniformly failed. Chemical and some successful FAB mass spectrometric analyses (see Experimental Section) provide good evidence for the formation of d^9–d^9 species. Evidence for Pd_2 bonds is furnished by the UV–visible spectra, in which the

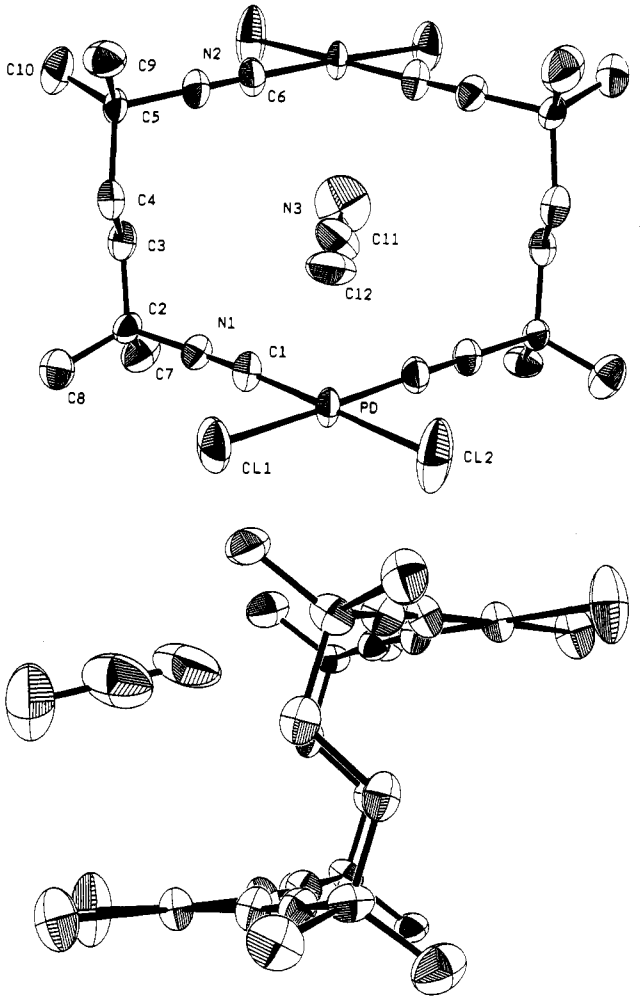

Figure 2. Molecular structure and atom labeling of *cis,cis*-$Pd_2(tmb)_2Cl_4 \cdot 2CH_3CN$, showing 50% probability ellipsoids (front (top) and side (bottom) view). For clarity, the hydrogen atoms have been omitted. Only one CH_3CN molecule is shown on this figure.

Scheme I

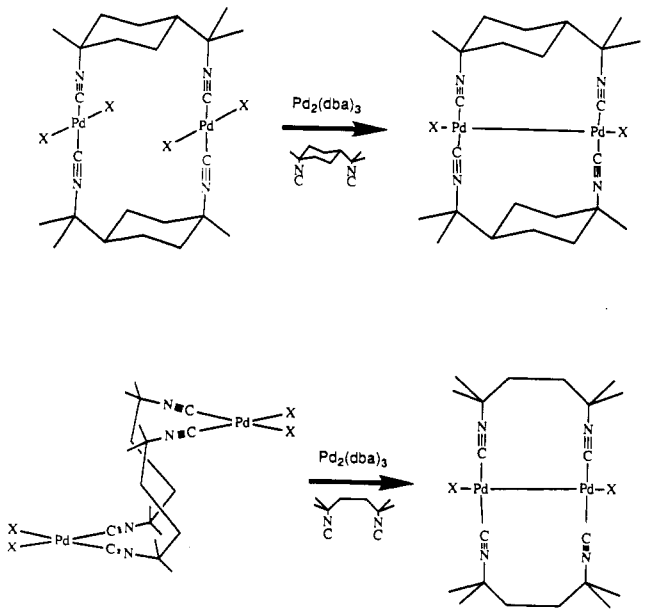

X = Cl, Br

M_2 $d\sigma \rightarrow d\sigma^*$ bands are identified in the 400–500 nm range ($3000 < \epsilon < 10000$ M^{-1} cm^{-1}; 298 K; CH_3CN).[18] In the Raman spectra

(15) Perreault, D.; Drouin, M.; Michel, A.; Harvey, P. D. *Inorg. Chem.* **1991**, *30*, 2.
(16) Miller, J. S., Ed. *Extended Linear Chain Compounds*; Plenum: New York, 1983; Vol. 1.
(17) Drouin, M.; Perreault, D.; Harvey, P. D.; Michel, A. *Acta Crystallogr.* **1991**, *C47*, 752.

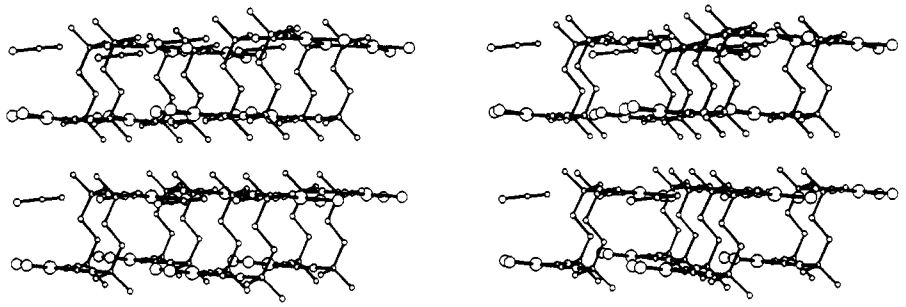

Figure 3. Stereoview of the crystal packing of *cis,cis*-$Pd_2(tmb)_2Cl_4 \cdot 2CH_3CN$.

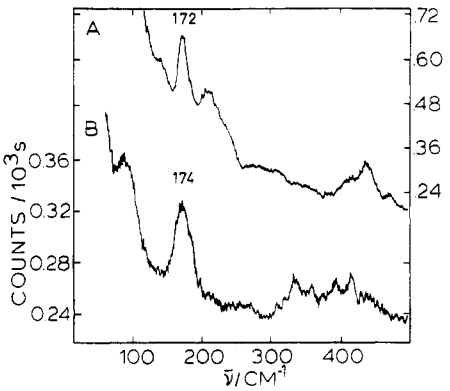

Figure 4. MicroRaman spectra of $Pd_2(tmb)_2Cl_2$ (A) and $Pd_2(dmb)_2Cl_2$ (B) in the solid state at 298 K. Laser excitation, 647 nm; laser power, 5 mW at the sample; number of scans, 1; 32×; 1 s/pt; 1-cm^{-1} step.

(λ_{exc} = 647, 752, 1064 nm), bands located at 172 and 174 cm^{-1} for $Pd_2(dmb)_2Cl_2$ and $Pd_2(tmb)_2Cl_2$, respectively, are selectively enhanced via preresonance effects (I(1064) < I(752) < I(647 nm)) and are assigned to $\nu(Pd_2)$ (Figure 4). These values compare favorably with those for the closely related d^9–d^9 species $Pd_2(CH_3NC)_6^{2+}$ (163)[19] and $Pd_2(dppm)_2Cl_2$ (152 cm^{-1}).[20] All attempts to obtain Raman spectra using 488.0- and 514.5-nm laser excitation failed as the samples undergo rapid, irreversible thermal (or photochemical) damage.

Although the preparation of these new d^9–d^9 species is essentially the same as that reported by Balch et al. during the mid 1970s,[21] using diphosphines and monodentate isocyanides the insertion of small molecules in the Pd_2 bond has not been observed yet.[22] The fundamental difference between the $Pd_2(dppm)_2X_2$ and $Pd_2(diiso)_2X_2$ (X = Cl, Br, I; diiso = dmb, tmb) complexes is that dppm, tmb, and dmb are three-, four-, and five-atom bridging ligands, respectively, and it is not clear whether an M_2 separation of 4.4 Å (see structure for $Pd_2(dmb)_2Cl_4$) could accommodate such insertions.

Despite the absence of crystal structure data, some comments can be made regarding the structures of the $Pd_2(diiso)_2X_2$ complexes. Distortions are expected, particularly for the $Pd_2(dmb)_2X_2$ complexes (X = Cl, Br). The $r(Rh_2)$ values for $Rh_2(tmb)_4^{2+}$ and $Rh_2(tmb)_4Cl_2^{2+}$ are 3.26 and 2.77 Å, respectively ($\Delta \sim 0.5$ Å),[23] while the Pd_2 bond length in d^9–d^9 species generally ranges between 2.6 and 2.7 Å.[24] The dmb ligand must accommodate a large change in bite distance from 2.7 to 4.4 Å in the $Pd_2(dmb)_2X_{2n}$ (n = 1, 2) complexes (Δ = 1.7 Å). This large change must be accompanied by observable molecular distortions. Indeed, the unreported structure of a closely related compound, $Ag_2(dmb)_2Br_2$[25] (structure II), exhibits a clear deviation of the AgCN angle (155°) from the ideal angle of 180° generally observed for terminal isocyanides. In $Ag_2(dmb)_2Br_2$, $r(Ag_2)$ is 3.345 (1) Å.[25a] Further molecular distortions can also be considered, notably within the dmb ligand. For instance, the bite distance measured in the Ag-encapsulated $[Ir_2Ag(dmb)_4]^{3+}$ complex (from an X-ray analysis), is ~5.2 Å[26] and appears to be the longest M–M distance to be reported so far. In addition, Sykes and Mann reported the structure for $[Ir_2(dmb)_4(PPh_3)(AuPPh_3)]^{3+}$ where $r(Ir_2)$ = 2.986 (2) Å.[13e] The published bite distances range from 3.0 to 5.2 Å and demonstrate the flexibility of the dmb ligand. Furthermore the $[Ir_2(dmb)_4(PPh_3)(AuPPh_3)]^{3+}$ structure exhibits a staggered conformation of the $Ir(CNR)_4$ planes to accommodate the shortened distance.[13e] It is believed that the $Pd_2(dmb)_2X_2$ complexes also experience a large dihedral angle between the C–Pd–C vectors. Because the $\nu(Pd_2)$ values (172 and 174 cm^{-1}) in the $Pd_2(diiso)_2Cl_2$ complexes are about the same, the $r(Pd_2)$ distances should also be similar, and under these conditions, the PdCN angle in the $Pd_2(dmb)_2X_2$ compounds (X = Cl, Br) must be smaller than that in the $Pd_2(tmb)_2X_2$ compounds. Such structural deformations may also be translated into ring stress in the d^9–d^9 species.

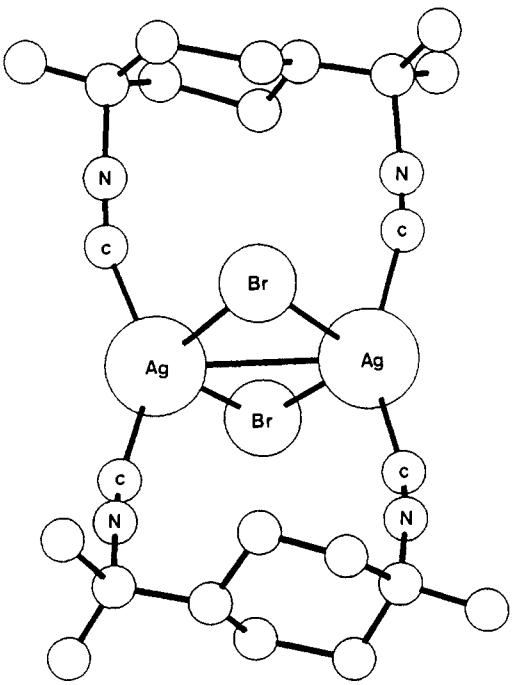

II

(18) Zietlow, M. Ph.D. Thesis, California Institute of Technology, 1989.
(19) Garciafigueroa, E.; Sourisseau, C. *Nouv. J. Chim.* **1978**, *2*, 593.
(20) Alves, O. L.; Vitorge, M.-C.; Sourisseau, C. *Nouv. J. Chim.* **1983**, *7*, 231.
(21) (a) Boehm, J. R.; Doonan, D. J.; Balch, A. L. *J. Am. Chem. Soc.* **1976**, *98*, 4845. (b) Benner, L. S.; Balch, A. L. *J. Am. Chem. Soc.* **1978**, *100*, 6099.
(22) Perreault, D.; Harvey, P. D. Unpublished results.
(23) Miskowski, V. M.; Smith, T. P.; Loehr, T. M.; Gray, H. B. *J. Am. Chem. Soc.* **1985**, *107*, 7925.
(24) Olmstead, M. M.; Benner, L. S.; Hope, H.; Balch, A. L. *Inorg. Chim. Acta* **1979**, *32*, 193.
(25) (a) Harvey, P. D.; Drouin, M.; Michel, A. Unpublished results. (b) A previously reported X-ray structure[25c] on $[Rh_2(dmb)_2(dppm)_2]^{2+}$ showed that the $r(Rh_2)$ value is 3.161 Å. The authors stated that the complex exhibits large bond angle distortions, notably for the C–Rh–C angle (169.7 (3)). (c) Boyd, D. C.; Matsch, P. A.; Mixa, M. M.; Mann, K. R. *Inorg. Chem.* **1986**, *19*, 3331.
(26) Sykes, A.; Mann, K. R. *J. Am. Chem. Soc.* **1988**, *110*, 8252.

Scheme II

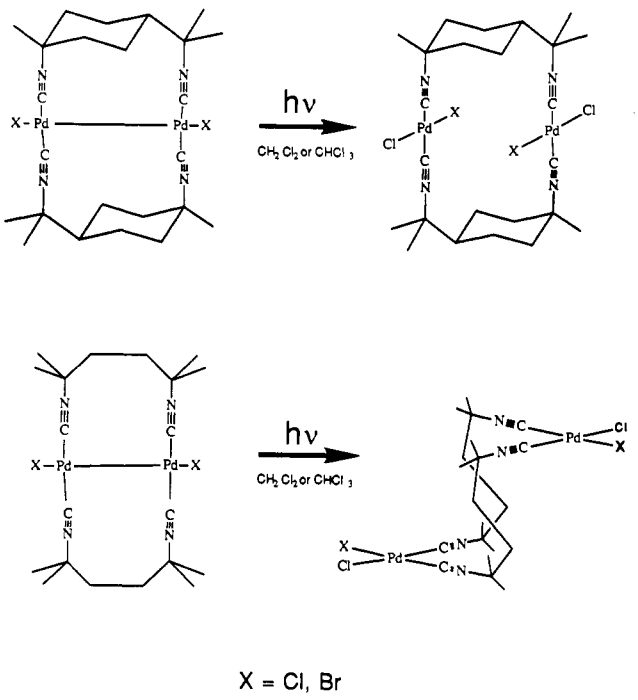

Scheme III

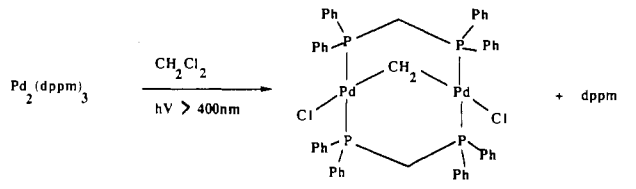

$Pd_2(diiso)_2X_2$ Photooxidation Reactions. The $Pd_2(diiso)_2X_2$ compounds (diiso = tmb, dmb; X = Cl, Br) are particularly photoreactive in neat $CHCl_3$ and CH_2Cl_2 solutions (under inert atmosphere). Monitoring the UV–visible spectra during the course of the photoreactions did not yield isosbestic points (250–800 nm) as the photoproducts are colorless or pale yellow. These photoproducts have been identified spectroscopically (^1H NMR, IR, UV–visible) by comparison with the $Pd_2(diiso)_2X_4$ compounds. The photoreactions proceed via an oxidative addition route as shown in Scheme II. In the $Pd_2(diiso)_2Br_2$ photoreactions, the mixed halide complexes are observed, and the $Pd_2(dmb)_2Br_2Cl_2$ product has been characterized by X-ray analysis (Table II). This compound is essentially isostructural to the $Pd_2(dmb)_2X_4$ analogues (X = Cl, I[12]) but X-ray analysis did not permit clear identification of the isomer formed (cis- or trans-$(Br)_2$) as statistical disorder is observed (see Experimental Section for details). These two-electron oxidative addition reactions differ from the reported efficient four-electron photooxidative addition of CH_2Cl_2 to $Pd_2(dppm)_3$ that forms the d^8–d^8 A-frame $Pd_2(dppm)_2(\mu\text{-}CH_2)Cl_2$ product (Scheme III).[27] Beside the difference in oxidation state of the Pd atoms in the starting materials, this difference appears to be due, in part, to an M_2 proximity factor in the case of the $Pd_2(dmb)_2X_2$ complexes; the M_2 separations in A-frame compounds range from 3.0 to 3.3 Å.[28] An A-frame photoproduct could have been expected for the $Pd_2(tmb)_2X_2$ (X = Cl, Br) reactions, but was not observed. Electronic factors could play a role in determining the structures of the photoproducts.

Table III. Photochemical Quantum Yields[a]

	$CHCl_3$	CH_2Cl_2		$CHCl_3$	CH_2Cl_2
$Pd_2(dmb)_2Cl_2$	0.41	0.12	$Pd_2(dmb)_2Br_2$	1.35	0.35
$Pd_2(tmb)_2Cl_2$	0.46	0.05	$Pd_2(tmb)_2Br_2$	0.19	0.12

[a] At 298 K; the experimental error is ±10%.

No attempt has been made to isolate and identify the highly diluted organic photoproducts resulting from the release of CH_2 and CHCl radicals. It is suspected that ethylene could be one of the products.[29,30]

The photochemical quantum yields (Φ) range from 0.05 to 1.35 (Table III), and an increase in Φ on going from CH_2Cl_2 to $CHCl_3$ as solvent is observed, which is consistent with a chlorine atom abstraction mechanism.[29a] In three out of four cases in Table III we observe $\Phi(Pd_2(diiso)_2Cl_2) < \Phi(Pd_2(diiso)_2Br_2)$, which is consistent with the better electron-donating ability of the Br atoms. Furthermore, the Φ value of 1.35 for $Pd_2(dmb)_2Br_2$ in $CHCl_3$ indicates that radical chain reactions take place, supporting the proposed mechanism. No study of the dependence of Φ on concentration was undertaken in this work. The greater Φ value for $Pd_2(tmb)_2Cl_2$ as compared to that for $Pd_2(tmb)_2Br_2$ in $CHCl_3$ remains unexplained.[29b]

Photoinduced oxidative addition reactivities in d^8–d^8 binuclear complexes are well known.[30] One important difference is that the nonmetal–metal-bonded M_2 d^8–d^8 compounds[30] photooxidatively add two Cl atoms with the formation of an M_2 bond (d^7–d^7), while in the d^9–d^9 species the photooxidative additions are accompanied by homolytic M_2 bond cleavage.

The second noticeable trend in Φ is that $\Phi(Pd_2(dmb)_2X_2) > \Phi(Pd_2(tmb)_2X_2)$ (X = Cl, Br),[31] with the exception of X = Cl in $CHCl_3$. This trend is attributed to a difference in ring stress between the dmb and tmb d^9–d^9 complexes, where the ring stress in the dmb complexes is likely to be greater than that for the tmb complexes (see previous section). This effect has important implications for the homolytic bond cleavage reactivities.

In this work, new M_2-bonded complexes have been prepared which afford the possibility of varying the axial ligands X (employing halogens or other two-electron donor ligands) in such a way that the photoinduced reactivities of the M_2 species could be changed.

Furthermore, the possibility of varying the bridging ligands should impose some favorable ring stress. In some cases, one may conceive structural designs which permit tuning of photochemical electron transfer reactivity. The results of the present study certainly show variations of the reactivity with changes in the axial and bridging ligands in most cases, but fine tuning has not been achieved in this work. The list of axial and bridging ligands will be extended in future investigations.

Acknowledgment. We thank NSERC, FCAR, and Bureau de la recherche (Université de Sherbrooke) for financial support. D.P. acknowledges the Université de Sherbrooke for a graduate fel-

(27) Caspar, J. V. *J. Am. Chem. Soc.* **1985**, *107*, 6718.

(28) (a) Colton, R.; McCormick, M. J.; Pannan, C. D. *Aust. J. Chem.* **1978**, *31*, 1425. (b) Khan, M. A.; McAlees, A. J. *Inorg. Chim. Acta* **1985**, *104*, 109. (c) Balch, A. L.; Benner, L. S.; Olmstead, M. M. *Inorg. Chem.* **1979**, *18*, 2996. (d) Balch, A. L.; Lee, C. S.; Lindsay, C. H.; Olmstead, M. M. *J. Organomet. Chem.* **1979**, *C22*, 177. (e) Cowie, M.; Dickson, R. S. *Inorg. Chem.* **1981**, *20*, 2682. (f) McKee, I. R.; Cowie, M. *Inorg. Chim. Acta* **1982**, *65*, L107. (g) Hanson, A. W.; McAlees, A. J.; Taylor, A. *J. Chem. Soc., Perkin Trans.* **1985**, 441.

(29) (a) See for example Laine, R. M.; Ford, P. C. *Inorg. Chem.* **1977**, *16*, 388. (b) The atom transfer mechanism appears to be a pre-eminent reaction pathway in binuclear systems.[30] The possibility of an electron transfer mechanism for these electron-rich d^9 species still exists. If two processes occur simultaneously for the $Pd_2(tmb)_2Cl_2/CHCl_3$ system, an increase in the Φ value could then be expected.

(30) (a) Roundhill, D. M.; Atherton, S. J. *Inorg. Chem.* **1986**, *25*, 4071. (b) See for example: Marshall, J. L.; Stiegman, A. E.; Gray, H. B. *Excited States and Reactive Intermediates: Photochemistry, Photophysics and Electrochemistry*; Lever, A. B. P., Ed.; ACS Symposium Series 307; American Chemical Society: Washington, DC, 1986; p 166. (c) Smith, D. C.; Gray, H. B. *Challenge of d and f Electrons*; Salahub, D. R., Zerner, M. C., Eds.; ACS Symposium Series No. 394; American Chemical Society: Washington, DC, 1989; p 356. (d) Meyer, T. J.; Caspar, J. V. *Chem. Rev.* **1985**, *85*, 187.

(31) For X = Cl and $CHCl_3$ as solvent, the Φ values are 0.41 and 0.46 for diiso = dmb and tmb, respectively (Table III). These values are equal within the experimental error (10%). Again the Φ value for $Pd_2(tmb)_2Cl_2$ in $CHCl_3$ is relatively high and additional factors are suspected to contribute to this high value.

lowship. P.D.H. is indebted to Mrs. R. Zamojska for the chemical analyses for Pd, Cl, and Br, and to Mr. Y. Huang (McGill University) for some of the Raman studies.

Supplementary Material Available: A complete table of crystal data for I, II, and III and tables of atomic positional parameters, bond distances, bond angles, anisotropic thermal parameters, and data collection parameters for $Pd_2(dmb)_2Cl_4 \cdot H_2O$, $Pd_2(tmb)_2Cl_4 \cdot 2CH_3CN$, and $Pd_2(dmb)_2Br_2Cl_2$ (14 pages); tables of observed and calculated structure factors for $Pd_2(dmb)_2Cl_4 \cdot H_2O$, $Pd_2(tmb)_2Cl_4 \cdot 2CH_3CN$, and $Pd_2(dmb)_2Br_2Cl_2$ (30 pages). Ordering information is given on any current masthead page.

Contribution from the Department of Chemistry,
Iowa State University, Ames, Iowa 50011-3111

Coordination Chemistry of a New Tetratertiary Phosphine Ligand

M. R. Mason, C. M. Duff, L. L. Miller, R. A. Jacobson, and J. G. Verkade*

Received June 28, 1991

The synthesis and characterization of the new tetratertiary phosphine 2,3-bis[(diphenylphosphino)methyl]-1,4-bis(diphenylphosphino)butane (**5**) is reported. Oxidation of **5** with *t*-BuOOH or S_8 yields the tetraphosphoryl and tetrathiophosphoryl derivatives **6** and **7**, respectively. The molecular structure of **6** was confirmed by X-ray crystallography. Crystals of **6** are triclinic, space group $P\bar{1}$, with unit cell dimensions a = 11.70 (3) Å, b = 21.80 (3) Å, c = 9.28 (6) Å, α = 94.0 (3)°, β = 102.7 (3)°, and γ = 88.4 (2)°. The complexes $[CH(CH_2PPh_2)_2ML_n]_2$ have been prepared for ML_n = $PdCl_2$, $PdBr_2$, PdI_2, $NiCl_2$, $PtCl_2$, $Cr(CO)_4$, $Mo(CO)_4$, $W(CO)_4$, and $Fe(CO)_3$, in which **5** coordinates in a bis(bidentate) manner to two metals with the formation of two six-membered chelate rings. This coordination mode was confirmed by single-crystal X-ray diffraction studies on the complexes $[CH(CH_2PPh_2)_2ML_n]_2$ for ML_n = $PdCl_2$ and $NiCl_2$. Crystals of $[CH(CH_2PPh_2)_2PdCl_2]_2$ are monoclinic, space group $P2_1/n$, with unit cell dimensions a = 21.798 (8) Å, b = 13.927 (5) Å, c = 22.802 (9) Å, and β = 115.81 (4)°. Crystals of $[CH(CH_2PPh_2)_2NiCl_2]_2$ are triclinic, space group $P\bar{1}$, with unit cell dimensions a = 14.320 (5) Å, b = 14.601 (2) Å, c = 19.448 (15) Å, α = 92.39 (2)°, β = 99.83 (4)°, γ = 99.00 (1)°, and Z = 4. The monometallic complex $(Ph_2P(O)CH_2)_2CHCH(CH_2PPh_2)_2PdCl_2$ was also synthesized. Crystals of this complex are orthorhombic, space group *Pna*2, No. 33, with unit cell dimensions a = 33.375 (5) Å, b = 11.125 (2) Å, c = 14.886 (3) Å, and Z = 4. The monometallic complexes (**5**-*P*,*P*′,*P*″)$Mo(CO)_3$ were prepared in which **5** exhibits a tridentate (*P*,*P*′,*P*″) coordination mode and where the fourth P of **5** can have a lone pair or be bonded to *O* or S in addition to two phenyl groups. The monometallic complex (**5**)RhCl was also prepared, but ^{31}P NMR spectroscopy indicated a complicated solution behavior for this complex. Similarly, attempted syntheses of monometallic complexes of Ni(II) and Pd(II) yielded mixtures which also exhibit complex behavior in solution as shown by ^{31}P NMR spectroscopy.

Introduction

Recently our group has been investigating the coordination chemistry of the main-group elements P, As, Si, and Ge with the tetrol frameworks **1a–1d**. These investigations have focused on the synthesis and reactivity of the orthoesters of these elements, such as phosphorus in **2a–2d**,[1] as well as the attempted synthesis

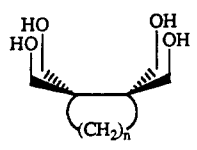

	n
1a	0
1b	1
1c	2
1d	3

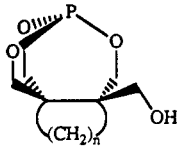

	n
2a	0
2b	1
2c	2
2d	3

of novel rectangular pyramidal five-coordinate species. Whereas five-coordinate phosphorus, arsenic, silicon, and germanium compounds typically favor a TBP geometry, the structural requirements of **1a–1d** are such that five-coordinate tetraalkoxide species of these elements must exhibit a SP geometry. As a step toward this goal we have recently reported the results of deprotonation studies of the pendant alcohol group of **2a–2d**[1,2] and the structures of the two novel silicon isomers **3a** and **3b**.[3]

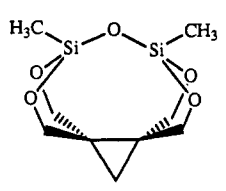

3a

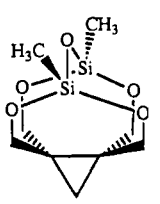

3b

We have now undertaken an elaboration of this project to include the chemistry of the transition-metal elements with donor atoms other than oxygen in **1a–1d**. Of present interest is the introduction of phosphine groups into the tetradentate framework. A tetradentate phosphine of this kind may exhibit any one of four possible coordination modes, A–D. One interesting possibility

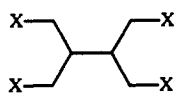

4 X = Cl
5 X = PPh_2
6 X = $P(O)Ph_2$
7 X = $P(S)Ph_2$

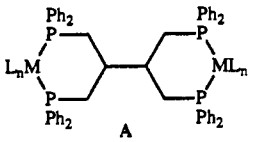

A

ML_n ML_n

8 $PdCl_2$	**14** $Mo(CO)_4$
9 $PdBr_2$	**15** $W(CO)_4$
10 PdI_2	**16** $Fe(CO)_3$
11 $NiCl_2$	
12 $PtCl_2$	
13 $Cr(CO)_4$	

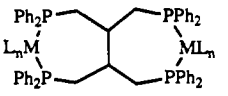

B

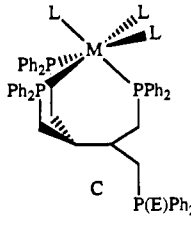

C

ML_3 = $Mo(CO)_3$

17 E = lone pair
18 E = O
19 E = S

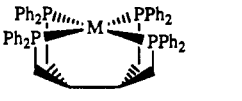

D

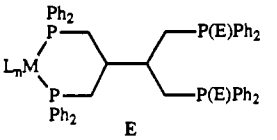

E

ML_n = $PdCl_2$

20 E = lone pair
21 E = O

(1) Davis, R. V.; Wintergrass, D. J.; Janakiraman, M. N.; Hyatt, E. M.; Jacobson, R. A.; Daniels, L. M.; Wroblewski, A.; Padmakumari Amma, J.; Das, S. K.; Verkade, J. G. *Inorg. Chem.* **1991**, *30*, 1330.
(2) Davis, R. V.; Verkade, J. G. *Inorg. Chem.* **1990**, *29*, 4983.
(3) de Ruiter, B.; Benson, J. E.; Jacobson, R. A.; Verkade, J. G. *Inorg. Chem.* **1990**, *29*, 1065.

0020-1669/92/1331-2746$03.00/0